



Journal of Applied and Computational Mechanics



Research Paper

Insight into Stability Analysis on Modified Magnetic Field of Radiative Non-Newtonian Reiner–Philippoff Fluid Model

Iskandar Waini¹, Abdul Rahman Mohd Kasim², Najiyah Safwa Khashi'ie¹, Nurul Amira Zainal¹, Anuar Ishak³, Ioan Pop⁴

¹ Fakulti Teknologi Kejuruteraan Mekanikal dan Pembuatan, Universiti Teknikal Malaysia Melaka, Hang Tuah Jaya, 76100 Durian Tunggal, Melaka, Malaysia

² Centre for Mathematical Sciences, College of Computing & Applied Sciences, Universiti Malaysia Pahang, Lebuhraya Tun Razak, Gambang 26300, Pahang, Malaysia

³ Department of Mathematical Sciences, Faculty of Science and Technology, Universiti Kebangsaan Malaysia, 43600 UKM Bangi, Selangor, Malaysia

⁴ Department of Mathematics, Babeş-Bolyai University, 400084 Cluj-Napoca, Romania

Received October 10 2021; Revised January 09 2022; Accepted for publication January 09 2022.

Corresponding author: A.R. Mohd Kasim (rahmanmohd@ump.edu.my)

© 2022 Published by Shahid Chamran University of Ahvaz

Abstract. The field of magnetohydrodynamics (MHD) encompasses a wide range of physical objects due to their stabilising effects. Thus, this study concerns the numerical investigation of the radiative non-Newtonian fluid flow past a shrinking sheet in the presence of an aligned magnetic field. By adopting proper similarity transformations, the governing partial derivatives of multivariable differential equations are converted to similarity equations of a particular form. The numerical results are obtained by using the *bvp4c* technique. According to the findings, increases in the suction parameter resulted in higher values of the skin friction and heat transfer rate. The same pattern emerges as the aligned angle and magnetic parameter are considered. On the other hand, the inclusion of the Bingham number, the Reiner–Philippoff fluid, and the thermal radiation parameters deteriorate the heat transfer performance, evidently. The dual solutions are established, which results in a stability analysis that upholds the validity of the first solution.

Keywords: Reiner–Philippoff fluid, shrinking sheet, aligned magnetic, heat transfer, stability analysis, thermal radiation.

1. Introduction

Magnetohydrodynamics (MHD), a subclass of physics, highlights the magnetic characteristic within electrically working fluids like electrolytes, plasmas, and liquid metals. Besides being one of the attractions in the fluid mechanic's research, MHD is practically embedded in electrostatic filters, heat exchangers, power pumps, and generators. The fundamental concept of MHD in fluid mechanics is related to the production of Lorentz force quantity, which obstructs the motion, hence, functional in suspending the separation from laminar to the turbulent boundary layer. The advantageous effect of MHD was highlighted by Rashidi et al. [1] in the creation of an energy generator. Sheikholeslami et al. [2] observed the fluid behavior and thermal progress in semi-annulus utilising magnetic field. According to Hussain et al. [3], the chemical reaction, Hall current, and MHD are the contributing factors in the development of fluid motion due to an accelerated moving plate. Haq et al. [4] analyzed the magnetic field with an aligned angle which led to the declination of the heat transfer quantity and the advancement of the skin friction coefficient. This observation was following the findings by Rashid et al. [5]. Recently, the aligned magnetic field of an upper-convected Maxwell fluid was studied by Bilal and Nazeer [6]. The significance of the MHD effect in the boundary layer flow analysis also can be accessed in the papers by Khashi'ie et al. [7, 8], Srinivasulu and Goud [9], Saranya and Al-Mdallal [10], Zhang et al. [11], Waini et al. [12–14] and Ali et al. [15–21].

The progressive growth in industrial and technological sectors is among the factors, which lead to the extensive attention for an effective working fluid especially in the manufacturing and engineering processes. The classical Newtonian base fluid like water is frequently unable to fulfill the industrial demands for example in the thermal performance. Hence, the various subclass of non-Newtonian fluids with different features like shear rate-dependent viscosity and normal stress, are widely used in lubricating and grease oils, pharmaceutical products, cosmetic products, biological fluids, food processing, and mineral suspensions. Unlike the Newtonian fluid model which is based on the linear relationship between strain and stress tensors, the non-Newtonian fluid models are observed based on their viscosity's behaviour either shear thickening (dilatant) or shear thinning (pseudo-plasticity). There are many proposed models with both shear thickening and thinning behaviors like the Reiner–Philippoff fluid, the Sisko fluid, Powell–Eyring fluid, Carreau–Yasuda fluid, and the Carreau viscosity fluid [22].



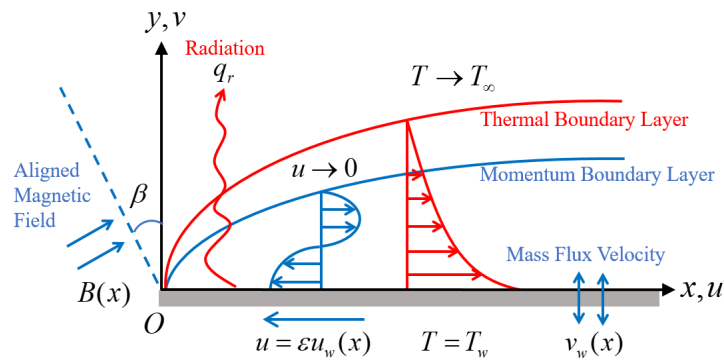


Fig. 1. Schematic configuration of flow.

The Reiner–Philippoff fluid model exhibits Newtonian fluid if the shear stress approaches zero or becomes large whilst for other values of shear stress, this fluid model can present the non-Newtonian fluid behavior. This is special characteristics of Reiner–Philippoff model and it can be generally used for both Newtonian and non-Newtonian type of fluid. Kapur and Gupta [23] scrutinized the Reiner–Philippoff fluid inside a channel when the shear stress parameters are large and small using Karman–Pohlhausen’s method. Meanwhile, Cavatorta and Tonini [24] compared the velocity profiles for non-Newtonian Reiner–Philippoff, Ellis, Ostwald de Waele, generalized Bingham and Prandtl Eyring fluids. Numerous studies were also conducted on the flow over a stretching surface in non-Newtonian fluids owing to their significance in many engineering and industrial processes. Previous analysis by Hansen and Na [25] revealed that the similarity solutions only exist when the non-Newtonian fluids (any model) flow over a 90° wedge. Later, Na [26] extended this study for the Blasius flow and the flow over a 90° wedge. Meanwhile, the flow in a three-dimensional system using a general non-Newtonian fluid model was studied and discussed by Timol and Kalthia [27], Patel and Timol [28], and Patil et al. [29]. Moreover, Yam et al. [30] analyzed the Reiner–Philippoff fluid flow induced by a stretching 90° wedge. Another interesting study by Ahmad et al. [31] was conducted for the Reiner–Philippoff fluids flow induced by the nonlinearly stretching sheet including the variable thickness effects. They established the skin friction as a constant function for a Newtonian fluid, a decreasing function for the shear-thinning case, and an increasing function for the shear-thickening case. Besides, Reddy et al. [32] numerically investigated the Reiner–Philippoff fluid flow in a Darcy–Forchheimer porous medium. They discovered that the temperature profile is an increasing function of the Reiner–Philippoff fluid parameter. This finding was also in accordance with the study by Kumar et al. [33]. Other interesting works on the flow of Reiner–Philippoff fluid were considered by Ahmad [34] with the thermophoresis and Brownian motion effects, Reddy et al. [35] with the MHD and the radiation effects, and Sajid et al. [36] with the variable species diffusivity and the heat source/sink effects.

Thus, while fulfilling the research gap, this numerical study is aim on the contribution to the dual solutions and stability analysis of non-Newtonian Reiner–Philippoff fluid flow and heat transfer over a shrinking sheet. In addition, the thermal radiation and the aligned magnetic field effects are considered. It is worth to mention that the present results have been undergoing validation process where the present model can be deduced to the available model in literature at some limiting cases. The reduced ordinary differential equations are numerically solved using the efficient bvp4c solver in the Matlab software and the similarity solutions are displayed and discussed. To the best of the authors’ knowledge, the study on the Reiner–Philippoff fluid flow over a shrinking sheet is limited and therefore, this endeavor is significant as a future reference to the practitioner, scientist, engineers as well as fluid mechanist and will be used as preliminary study on the real applications.

2. Mathematical Formulation

Consider the flow of Reiner–Philippoff fluid over a shrinking sheet as presented in Fig. 1. Here, the surface velocity is $u_w(x) = ax^{1/3}$ with $a > 0$. In addition, the mass flux velocity, $v_w(x)$ is considered to represent the surface permeability. Besides, the magnetic field $B(x) = B_0x^{-1/3}$ with the aligned angle β is employed where B_0 is constant magnetic strength. The idea on the similar study on the transverse magnetic toward the flow can be found in report by Reddy et al. [35]. Furthermore, the radiative heat flux $q_r = -(4\sigma^*/3k^*)(\partial T^4/\partial y)$ is also considered. Here, k^* and σ^* signifies the mean absorption and the Stefan-Boltzmann constants and given that $T^4 \cong 4T_\infty^3 T - 3T_\infty^4$ [37].

Therefore, the governing equations are [5, 35]:

$$\frac{\partial u}{\partial x} + \frac{\partial v}{\partial y} = 0 \tag{1}$$

$$\frac{\partial u}{\partial y} = \frac{\tau}{\mu_\infty + \frac{\mu_0 - \mu_\infty}{1 + \left(\frac{\tau}{\tau_s}\right)^2}} \tag{2}$$

$$u \frac{\partial u}{\partial x} + v \frac{\partial u}{\partial y} = \frac{1}{\rho} \frac{\partial \tau}{\partial y} - \frac{\sigma}{\rho} B^2 \sin^2(\beta) u \tag{3}$$

$$u \frac{\partial T}{\partial x} + v \frac{\partial T}{\partial y} = \left(\frac{k}{\rho C_p} + \frac{16\sigma^* T_\infty^3}{3(\rho C_p) k^*} \right) \frac{\partial^2 T}{\partial y^2} \tag{4}$$



subject to:

$$\begin{aligned} u &= \varepsilon u_w(x), \quad v = v_w(x), \quad T = T_w \quad \text{at } y = 0; \\ u &\rightarrow 0, \quad T \rightarrow T_\infty \quad \text{as } y \rightarrow \infty \end{aligned} \quad (5)$$

where σ is the electric conductivity, ρ is the fluid density, k is the thermal conductivity, ρC_p is the heat capacity, T is the temperature with the surface temperature T_w and the ambient temperature T_∞ , and (u, v) be the velocity components in the (x, y) direction. Besides, τ is the shear stress of the Reiner–Philippoff fluid model with the reference shear stress τ_s , the limiting dynamic viscosity μ_∞ , and the zero-shear dynamic viscosity μ_0 where it once mentioned by Yam et al. [30]. Whereas, the term ε in boundary condition (5) representing the parameter of stretching/ shrinking.

The similarity solutions are only existed by employing the similarity transformation (see Refs. [30, 35]):

$$\psi = \sqrt{a\nu}x^{2/3}f(\eta), \quad \tau = \rho\sqrt{a^3\nu}g(\eta), \quad \theta(\eta) = \frac{T - T_\infty}{T_w - T_\infty}, \quad \eta = \frac{y}{x^{1/3}}\sqrt{\frac{a}{\nu}} \quad (6)$$

where the stream function ψ is defined by $u = \partial\psi/\partial y$ and $v = -\partial\psi/\partial x$. Then:

$$u = ax^{1/3}f'(\eta), \quad v = -\sqrt{a\nu}x^{-1/3}\left(\frac{2}{3}f(\eta) - \frac{1}{3}\eta f'(\eta)\right) \quad (7)$$

By setting $\eta = 0$, the wall mass flux velocity becomes:

$$v_w(x) = -\frac{2}{3}\sqrt{a\nu}x^{-1/3}S \quad (8)$$

where $f(0) = S$ signify the constant mass flux parameter which represent suction strength ($S > 0$) and impermeable surface ($S = 0$), and $\nu = \mu_\infty/\rho$ is the fluid kinematic viscosity. Then, on using Eqs. (6) and (7), the similarity equations are obtained as follows:

$$g = f'' \left(\frac{\lambda\gamma^2 + g^2}{\gamma^2 + g^2} \right) \quad (9)$$

$$g' + \frac{2}{3}ff'' - \frac{1}{3}f'^2 - M\sin^2(\beta)f' = 0 \quad (10)$$

$$\frac{1}{Pr} \left(1 + \frac{4}{3}R \right) \theta'' + \frac{2}{3}f\theta' = 0 \quad (11)$$

subject to:

$$\begin{aligned} f(0) &= S, \quad f'(0) = \varepsilon, \quad \theta(0) = 1; \\ f'(\eta) &\rightarrow 0, \quad \theta(\eta) \rightarrow 0 \quad \text{as } \eta \rightarrow \infty \end{aligned} \quad (12)$$

with the Reiner–Philippoff fluid parameter λ , the Bingham number γ , the magnetic parameter M , the Prandtl number Pr , and the thermal radiation parameter R which are defined by:

$$\lambda = \frac{\mu_0}{\mu_\infty}, \quad \gamma = \frac{\tau_s}{\rho\sqrt{a^3\nu}}, \quad M = \frac{\sigma}{\rho a} B_0^2, \quad Pr = \frac{\rho C_p}{k}, \quad R = \frac{4\sigma^* T_\infty^3}{kk'} \quad (13)$$

Note that, $\lambda = 1$ is for the Newtonian (constant viscosity) fluid case, while $\lambda < 1$ and $\lambda > 1$ represent the shear thickening (dilatant) fluid and the shear-thinning (pseudoplastic) fluid cases. Besides, $\varepsilon = 0$ denotes the static sheet, while $\varepsilon > 0$ and $\varepsilon < 0$ signify the stretching and shrinking sheets, respectively.

The physical quantity of C_f and Nu_x are

$$C_f = \frac{\tau_w}{\rho u_w^2}, \quad Nu_x = \frac{xq_w}{k(T_w - T_\infty)} \quad (14)$$

where:

$$\tau_w = \rho\sqrt{a^3\nu}(g(\eta))_{y=0}, \quad q_w = -k \left(\frac{\partial T}{\partial y} \right)_{y=0} + (q_r)_{y=0} \quad (15)$$

Here, τ_w denotes the value of τ on $y = 0$ and q_w is the surface heat flux. On using Eqs. (14) and (15), one gets:

$$Re_x^{1/2}C_f = g(0), \quad Re_x^{-1/2}Nu_x = -\left(1 + \frac{4}{3}R\right)\theta'(0) \quad (16)$$

where local Reynolds number defines as $Re_x = u_w(x)x/\nu$.

3. Stability Analysis

The dual solutions are examined to test their stability by employing stability analysis [38, 39]. The solutions of the similarity equations do not have to be unique for given initial and boundary conditions because of the nonlinearity of the differential



equations, variation of geometric or fluid mechanical parameters. These can lead to bifurcations in the solution and thus to multiple solutions. In steady flows, there are frequently multiple solutions when flow separation or backflow occurs. One of the solutions is frequently a flow attached to the body, whereas the other solutions describe flow with separation. In these solutions, some have physical significance or are stable and others are unstable. Therefore, to check which solution is stable or physical reliable, the stability analysis must be conducted as explained by Merkin [38] and Weidman et al. [39]. Also, the suitable values of parameters can be determined to avoid misjudgement in flow and heat transfer analysis. In this regard, consider the semi-similar variables as follows [30]:

$$\psi = \sqrt{a\nu}x^{2/3}f(\eta, \Gamma), \quad \tau = \rho\sqrt{a^3\nu}g(\eta, \Gamma), \quad \theta(\eta, \Gamma) = \frac{T - T_\infty}{T_w - T_\infty}, \quad \eta = \frac{y}{x^{1/3}}\sqrt{\frac{a}{\nu}}, \quad \Gamma = \frac{a}{x^{2/3}}t \quad (17)$$

where Γ is the dimensionless time variable, and given that:

$$u = \alpha x^{1/3} \frac{\partial f}{\partial \eta}(\eta, \Gamma), \quad (18)$$

$$v = -\sqrt{a\nu}x^{-1/3} \left(\frac{2}{3}f(\eta, \Gamma) - \frac{1}{3}\eta \frac{\partial f}{\partial \eta}(\eta, \Gamma) - \frac{2}{3}\Gamma \frac{\partial f}{\partial \Gamma}(\eta, \Gamma) \right)$$

The use of Γ is associated with an initial value problem and is consistent with the equation of which solution will be obtained in practice as time evolves.

Next, consider the unsteady flow for Eqs. (2) and (3). Then, on using Eqs. (17) and (18), one obtains:

$$g = \frac{\partial^2 f (\lambda\gamma^2 + g^2)}{\partial \eta^2 (\gamma^2 + g^2)} \quad (19)$$

$$\frac{\partial g}{\partial \eta} + \frac{2}{3}f \frac{\partial^2 f}{\partial \eta^2} - \frac{1}{3} \left(\frac{\partial f}{\partial \eta} \right)^2 - M \sin^2(\beta) \frac{\partial f}{\partial \eta} - \frac{\partial^2 f}{\partial \eta \partial \Gamma} - \frac{2}{3}\Gamma \left(\frac{\partial f}{\partial \Gamma} \frac{\partial^2 f}{\partial \eta^2} - \frac{\partial f}{\partial \eta} \frac{\partial^2 f}{\partial \eta \partial \Gamma} \right) = 0 \quad (20)$$

$$\frac{1}{Pr} \left(1 + \frac{4}{3}R \right) \frac{\partial^2 \theta}{\partial \eta^2} + \frac{2}{3}f \frac{\partial \theta}{\partial \eta} - \frac{\partial \theta}{\partial \Gamma} - \frac{2}{3}\Gamma \left(\frac{\partial f}{\partial \Gamma} \frac{\partial \theta}{\partial \eta} - \frac{\partial f}{\partial \eta} \frac{\partial \theta}{\partial \Gamma} \right) = 0 \quad (21)$$

subject to:

$$f(0, \Gamma) - \frac{2}{3}\Gamma \frac{\partial f}{\partial \Gamma}(0, \Gamma) = S, \quad \frac{\partial f}{\partial \eta}(0, \Gamma) = \varepsilon, \quad \theta(0, \Gamma) = 1; \quad (22)$$

$$\frac{\partial f}{\partial \eta}(\eta, \Gamma) \rightarrow 0, \quad \theta(\eta, \Gamma) \rightarrow 0 \quad \text{as } \eta \rightarrow \infty$$

Then, consider the perturbation function [39]:

$$f(\eta, \Gamma) = f_0(\eta) + e^{-\alpha\Gamma}F(\eta, \Gamma),$$

$$g(\eta, \Gamma) = g_0(\eta) + e^{-\alpha\Gamma}G(\eta, \Gamma), \quad (23)$$

$$\theta(\eta, \Gamma) = \theta_0(\eta) + e^{-\alpha\Gamma}H(\eta, \Gamma)$$

where $F(\eta, \Gamma)$, $G(\eta, \Gamma)$, and $H(\eta, \Gamma)$ are arbitrary functions and relatively small rather than that $f_0(\eta)$, $g_0(\eta)$, and $\theta_0(\eta)$, and α denotes the eigenvalue. Here, Eq. (23) is employed to obtain the eigenvalue problems of Eqs. (19)-(21). By setting $\Gamma = 0$, then $F(\eta, \Gamma) = F_0(\eta)$, $G(\eta, \Gamma) = G_0(\eta)$ and $H(\eta, \Gamma) = H_0(\eta)$. Therefore, after linearization, the eigenvalue problems are:

$$G_0 = F_0'' \left(\frac{\lambda\gamma^2 + g_0^2}{\gamma^2 - 2f_0''g_0 + 3g_0^2} \right) \quad (24)$$

$$G_0' + \frac{2}{3}(f_0F_0'' + f_0''F_0) - \frac{2}{3}f_0'F_0' - M \sin^2(\beta)F_0' + \alpha F_0' = 0 \quad (25)$$

$$\frac{1}{Pr} \left(1 + \frac{4}{3}R \right) H_0'' + \frac{2}{3}(f_0H_0' + \theta_0'F_0) + \alpha H_0 = 0 \quad (26)$$

subject to:

$$F_0(0) = 0, \quad F_0'(0) = 0, \quad H_0(0) = 0;$$

$$F_0'(\eta) \rightarrow 0, \quad H_0(\eta) \rightarrow 0 \quad \text{as } \eta \rightarrow \infty \quad (27)$$

Here, to obtain α from Eqs. (24)-(26), $F_0'(\eta) \rightarrow 0$ as $\eta \rightarrow \infty$ in Eq. (27) is replaced by $F''(0) = 1$ [40].

4. Results and Discussion

This segment delivers a detailed discussion of the output attained from the numerical computations on Eqs. (9)-(12) using `bvp4c` package in the MATLAB software [41]. The analysis covers the discussions on the consequence of numerous physical parameters that arise in the proposed model where the outputs of the computations are presented in graphical and tabular form.



Table 1. Values of $f''(0)$ for different S when $\varepsilon = \lambda = \gamma = 1$ and $M = \beta = 0$

S	Cortell [42]	Ferdows et al. [43]	Waini et al. [44]	Present Result
-0.5	-0.518869	-0.518869	-0.518869	-0.518869
0	-0.677647	-0.677648	-0.677648	-0.677648
0.5	-0.873627	-0.873643	-0.873643	-0.873643

Table 2. Values of $-\theta'(0)$ for R and S when $\varepsilon = \lambda = \gamma = 1$, $M = \beta = 0$, and $Pr = 2$

R	S	Cortell [42]	Ferdows et al. [43]	Waini et al. [44]	Present Result
0	-0.5	0.3989462	0.398951	0.399100	0.399100
	0	0.7643554	0.764374	0.764357	0.764357
	0.5	1.2307661	1.230952	1.230792	1.230792
1	-0.5	0.2873762	0.287483	0.287485	0.287484
	0	0.4430879	0.443323	0.443323	0.443323
	0.5	0.6322154	0.632199	0.632200	0.632200

Table 3. Values of $g(0)$ for γ and λ when $S = M = \beta = 0$ and $\varepsilon = 1$

γ	λ	Sajid et al. [36]	Present Result
0.1	0.1	-0.660273	-0.660275
0.5	0.1	-0.380604	-0.380604
	1	-0.246415	-0.246415
0.1	0.3	-0.664497	-0.664498
	0.5	-0.668484	-0.668486
	0.7	-0.672282	-0.672277

Table 4. Values of $Re_x^{1/2}C_f$ and $Re_x^{-1/2}Nu_x$ for various values of physical parameters

ε	S	λ	γ	M	β	R	Pr	$Re_x^{1/2}C_f$	$Re_x^{-1/2}Nu_x$	
-1	2.4	1.5	0.1	0.02	$\pi/6$	3	10	1.115951	14.185386	
-0.5								0.708551	15.230413	
1								-1.868267	17.224642	
-1	2.33							0.962845	13.531937	
								1.050719	13.837810	
								1.085583	14.014575	
		2.4	0.5						1.165488	14.238467
									1.144604	14.215160
									1.057783	14.129413
			1.5	0.12					1.104794	14.173568
									1.083317	14.150968
									1.050718	14.117468
							0		1.102980	14.176042
				0.01				1.109615	14.180845	
				0.015				1.112818	14.183146	
				0.02	0			1.102980	14.176042	
					$\pi/3$			1.138984	14.201550	
					$\pi/2$			1.149432	14.208711	
					$\pi/6$	0		1.115951	15.591431	
						1		1.115951	15.077851	
						2		1.115951	14.608048	
						3	3	1.115951	3.592244	
							5	1.115951	6.486673	
							7	1.115951	9.520203	

To certify the reliability of the present model, a direct comparative study is performed on the existing value of $f''(0)$ and $-\theta'(0)$ reported by Cortell [42], Ferdows et al. [43], and Waini et al. [44]. Note that for the limiting case, the equations on the present model were identical and hence the comparison between the present results to the existing output is appropriate. The representation of validation data on the values of $f''(0)$ and $-\theta'(0)$ were tabulated in Tables 1 and 2, respectively.

The comparison shows an excellent agreement and hence gives confidence on the present mathematical formulation and the numerical consequences presented. To strengthen the present formulation as well as the present output, the values of $g(0)$ are also compared with the output reported by Sajid et al. [36] for different values of the Reiner–Philippoff fluid parameter λ and the Bingham number γ . The comparison shows a strong agreement, and hence the respective numerical values are presented in Table 3. It is seen that the values of $g(0)$ are increased significantly for larger values of γ . However, a small decrement is observed on the values of $Re_x^{1/2}C_f$ with the rise of λ .

Table 4 is presented to get an insight into the effect of parameters towards the variations of $Re_x^{1/2}C_f$ and $Re_x^{-1/2}Nu_x$ where the novelty and main contribution in the model development is highlighted. On the certain parameter investigated the fixed value has been used as $\varepsilon = -1$, $S = 2.4$, $\lambda = 1.5$, $\gamma = 0.1$, $M = 0.02$, $\beta = \pi/6$, $R = 3$, and $Pr = 10$. It is perceived that the values of $Re_x^{1/2}C_f$ are increased for the shrinking sheet ($\varepsilon = -1$) and showing the positive values, while the negative values of $Re_x^{1/2}C_f$ are obtained for the stretching sheet ($\varepsilon = 1$).



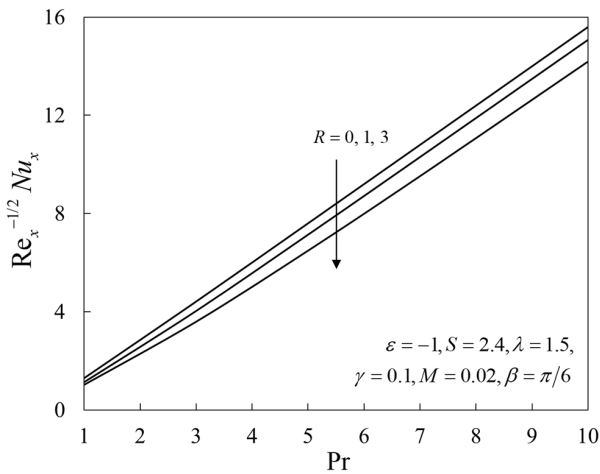


Fig. 2. $Re_x^{-1/2} Nu_x$ vs Pr and R

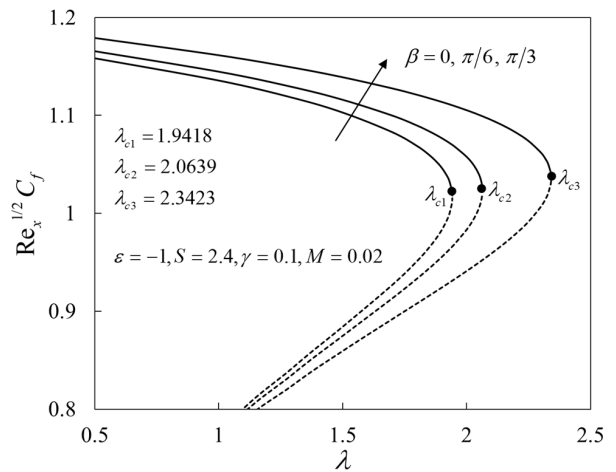


Fig. 3. $Re_x^{1/2} C_f$ vs λ and β

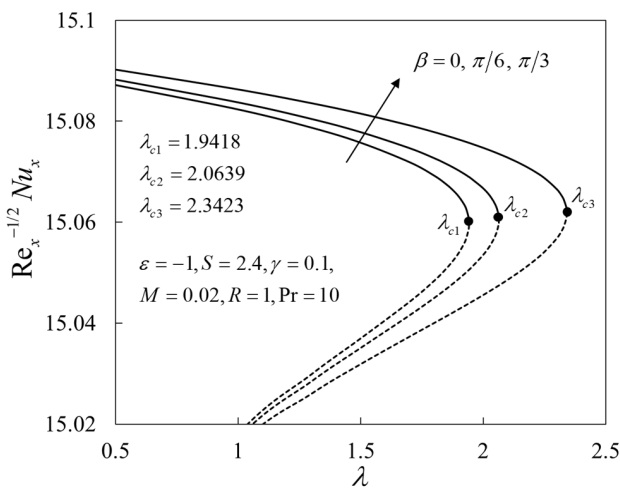


Fig. 4. $Re_x^{-1/2} Nu_x$ vs λ and β

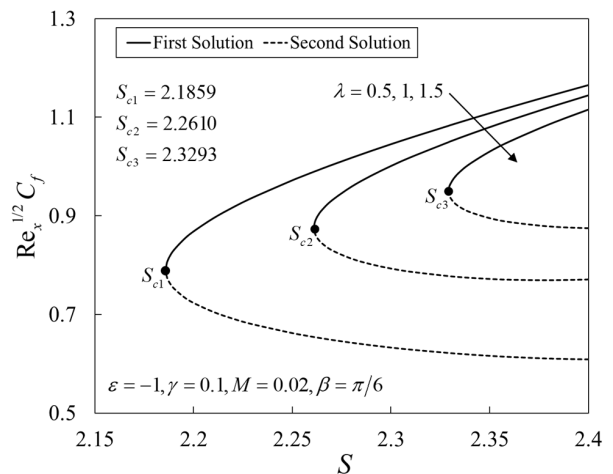


Fig. 5. $Re_x^{1/2} C_f$ vs S and λ

It is expected that the values of $Re_x^{1/2} C_f$ are higher in the shrinking environment due to the larger drag force developed on the shrinking surface. Meanwhile, the value of $Re_x^{-1/2} Nu_x$ significantly increased in the transition from shrinking to stretching region. A rise of S, M, and β led to boost the values of $Re_x^{1/2} C_f$, nonetheless contradictory behavior is observed for increasing in γ and λ . The values of $Re_x^{1/2} C_f$ remain unchanged for R and Pr due to the nonexistence term in the momentum equation, see Eq. (10). The increment in $Re_x^{-1/2} Nu_x$ are noticed for larger values of S, M, β , and Pr, whereas they are declining for λ , γ , and R. Physically, the increasing in $Re_x^{-1/2} Nu_x$ generally due to the augmentation in the movement of particles of fluid which developed the high rate of convective activities and hence established the larger heat transfer coefficient. However, the behavior might contradict if the bundle of external forces is involved simultaneously. The properties showed from the pertinent parameters will be considered as the controller of the certain processes.

The illustration on the effects of Pr and R towards the value of $Re_x^{-1/2} Nu_x$ can be seen in Fig. 2. The larger of Pr contributes to the increment of $Re_x^{-1/2} Nu_x$ but contradict behaviour is seen for larger value of R. Obviously, the bigger values of Pr aiding to the dominant convection process on flow mean the heat transfer is ideal to transpire by fluid momentum reasonably than fluid conduction. The strong value of R in fluid flow was remarked to restrict the heat transfer emitted which led to lesser values of $Re_x^{-1/2} Nu_x$. It is worth to highlight here, the Pr = 10 is used for other computation to meet the fact that the proposed model is under non-Newtonian type.

Figures 3 and 4 illustrated the dual solutions of $Re_x^{1/2} C_f$ and $Re_x^{-1/2} Nu_x$ for variations of λ and β , respectively. Noticeably, the values of λ are restricted for the shrinking sheet. The dual solutions are obtained up to the critical values $\lambda_{c1} = 1.9418$ in the absence of the magnetic field ($\beta = 0$), $\lambda_{c2} = 2.0639$ for $\beta = \pi/6$, and $\lambda_{c3} = 2.3423$ for $\beta = \pi/3$. The values of $Re_x^{1/2} C_f$ are significantly reduced as λ increased. It is logical because in the shear-thinning properties ($\lambda > 1$) the viscosity of the fluid is reducing which led to minimizing the contact of the fluid with the surface and the forces produced also condensed. The rate of heat transfer $Re_x^{-1/2} Nu_x$ also continuing to decrease for a poorly viscous fluid. Moreover, the values of $Re_x^{1/2} C_f$ and $Re_x^{-1/2} Nu_x$ are enhanced for larger β . The presence of β as an acute angle generally supports the strength of the magnetic field M. The stronger magnet strength developed sturdy Lorentz force which led to an upsurge in the skin friction as well as heat transfer rate. However, the results for the second solution is in disagreement with the first solution.

Figures 5 and 6 clarify the variations of $Re_x^{1/2} C_f$ and $Re_x^{-1/2} Nu_x$ against S for three different fluids which are the shear-thickening ($\lambda < 1$), the Newtonian ($\lambda = 1$), and the shear-thinning ($\lambda > 1$) fluids when $\epsilon = -1$, $\gamma = 0.1$, $M = 0.02$, and $\beta = \pi/6$. From these figures, the shear-thickening fluid ($\lambda = 0.5$) has the lowest critical value with $S_{c1} = 2.1859$, followed by the Newtonian fluid ($\lambda = 1$) with $S_{c2} = 2.2610$, and the shear-thinning fluid ($\lambda = 1.5$) with $S_{c3} = 2.3293$. This indicates the different types of fluid affect the boundary layer separation contrarily. In the engineering processes, this phenomenon is very important in order to certify the good end product on certain productions. The achieved critical values are typically famed as the separation value from laminar to turbulent boundary layer flow. In this case, when the critical value or point is attained, then the processes



on the certain production can be planned according to the output desire and the optimize productivity will be achieved. Besides, Figs. 3 and 4 also captured the second solutions of $Re_x^{1/2}C_f$ and $Re_x^{-1/2}Nu_x$, respectively. As the values of S increased, the first solution on both physical quantities $Re_x^{1/2}C_f$ and $Re_x^{-1/2}Nu_x$ are detected to enhance. Meanwhile, the second solution of $Re_x^{1/2}C_f$ significantly reduced and the increment of $Re_x^{-1/2}Nu_x$ is observed for larger S .

The obtained second solution correspondingly reflects the velocity and temperature profile as exemplified in Figs. 7 and 8 where the dual profiles are also achieved. The profiles show that the increase in λ reduces the velocity of the fluid for first solution. On the other hand, the second solution denies the behaviour. The reverse behaviour is attained for the temperature profiles. Both profiles presented are satisfied asymptotically at far-field boundary conditions.

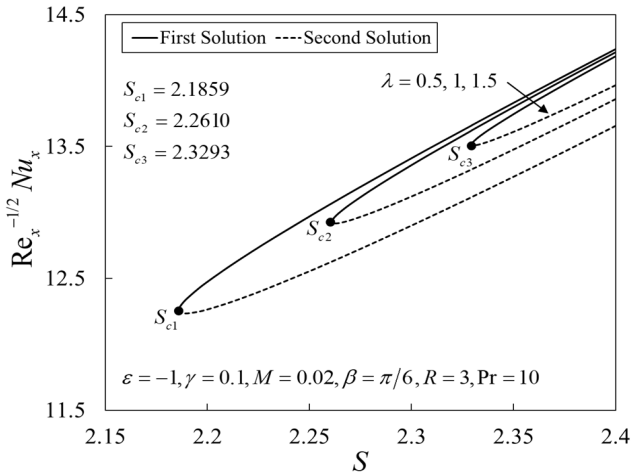


Fig. 6. $Re_x^{-1/2} Nu_x$ vs S and λ

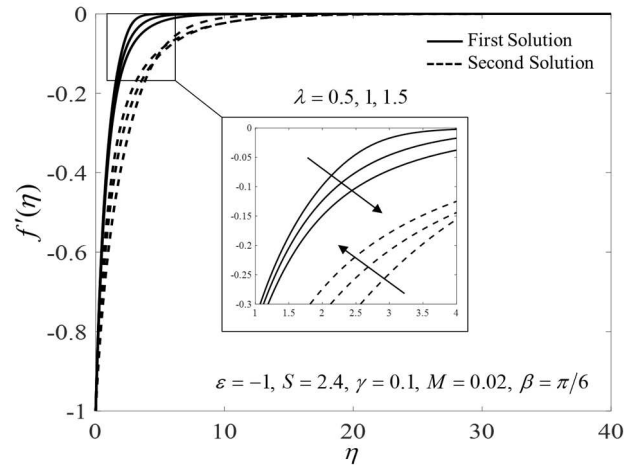


Fig. 7. $f'(\eta)$ vs λ

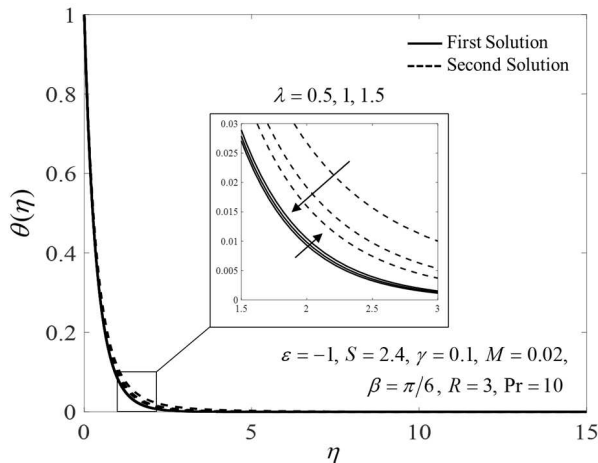


Fig. 8. $\theta(\eta)$ vs λ

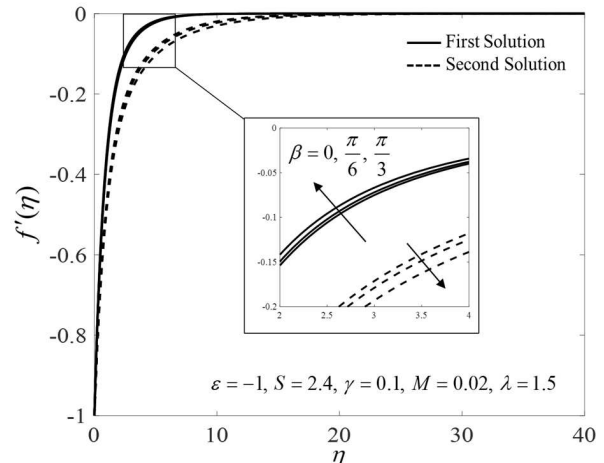


Fig. 9. $f'(\eta)$ vs β

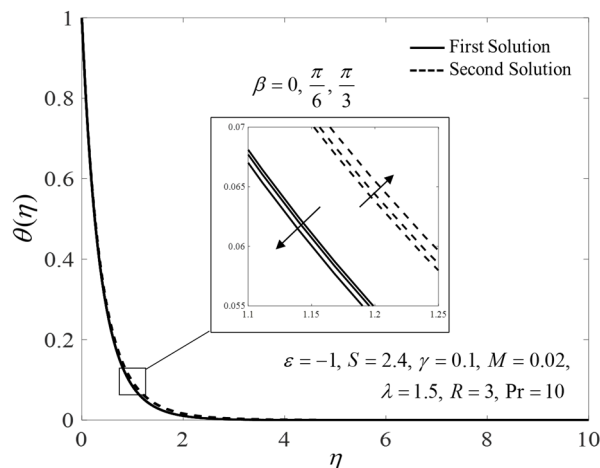


Fig. 10. $\theta(\eta)$ vs β

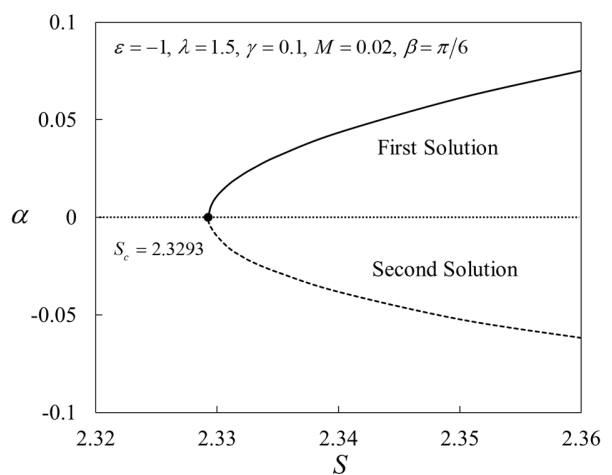


Fig. 11. α vs S



The distribution on velocity and temperature of fluid for various value β are illustrated in Figs. 9 and 10 respectively. It is clearly captured that, for large value of β , the first solution of fluid's velocity is increasing while decreasing for second solution. However, the contradict behavior is found for temperature distribution. Similar to profile in Figs, 7 and 8, both of the profiles against the value of β are also satisfied asymptotically at far-field boundary conditions.

Figure 10 presents the deviations of the smallest eigenvalues α versus S where the positive eigenvalue stands for the first solution, while the negative eigenvalue for the second solution. Hence, it can be decided that the significantly realizable solution is shown by the first solution and while the opposite manner by the second solution.

5. Conclusion

In the present article, an analysis of the radiative non-Newtonian fluid flow past a shrinking sheet with the aligned magnetic effect was considered mathematically. By using the boundary layer approach and suitable similarity transformations, the governing equations for the proposed model are reduced to ordinary differential equations. Physical features such as the friction factors and the heat transfer rate of the involved parameters are presented and discussed. The thermal rate is improved with the rise of the suction parameter and the Prandtl number. In addition, it has been demonstrated that increasing the magnetic parameter and the aligned angle improves thermal performance. The increase in the Bingham number and the Reiner-Philippoff fluid parameter appears to decrease the friction factor and the thermal rate. Meanwhile, the thermal efficiency is continuously reduced with the addition of the thermal radiation parameter. According to the stability analysis, the significantly realizable solution is shown by the first solution and while the opposite manner by the second solution. In summation, the highlight on the present work are as follows

- i. The non-Newtonian Reiner-Philippoff fluid flow past a nonlinearly shrinking sheet with an aligned magnetic field is studied.
- ii. The governing equations of the problem are transformed to the similarity equations and solved numerically using the `bvp4c` function in Matlab software.
- iii. Higher values of the skin friction coefficient and the heat transfer rate are attained as the aligned angle increase.
- iv. A temporal stability analysis is performed to determine the stability of the dual solutions.

Author Contributions

I. Waini developed the mathematical modelling, scheme, code of the problem, examined theory validation and writing the original manuscript; A.R. Mohd Kasim carried out the solution procedure and interpretation of the results; N.S. Khashi'ie and N.A. Zainal performed the stability analysis; A. Ishak and I. Pop conducted the parametric analysis, review and editing. The manuscript was written through the contribution of all authors. All authors discussed the results, reviewed and approved the final version of the manuscript.

Acknowledgments

The authors are very much thankful to the unknown reviewers for their valuable and constructive suggestions which improved the readability of the paper. Universiti Malaysia Pahang and Universiti Teknikal Malaysia Melaka are gratefully acknowledged.

Conflict of Interest

The authors declared no potential conflicts of interest with respect to the research, authorship and publication of this article.

Funding

The financial supports received from the Ministry of Higher Education (Project Code: RACER/1/2019/STG06/UMP//1) and Universiti Malaysia Pahang (Project Code: RDU213206).

Data Availability Statements

The datasets generated and/or analyzed during the current study are available from the corresponding author on reasonable request.

References


- [1] Rashidi, M.M., Abelman, S., Mehr, N.F., Entropy generation in steady MHD flow due to a rotating porous disk in a nanofluid, *International Journal of Heat and Mass Transfer*, 62, 2013, 515–525.
- [2] Sheikholeslami, M., Gorji-Bandpy, M., Ganji, D.D., MHD free convection in an eccentric semi-annulus filled with nanofluid, *Journal of the Taiwan Institute of Chemical Engineers*, 45, 2014, 1204–1216.
- [3] Hussain, S.M., Jain, J., Seth, G.S., Rashidi, M.M., Free convective heat transfers with hall effects, heat absorption and chemical reaction over an accelerated moving plate in a rotating system, *Journal of Magnetism and Magnetic Materials*, 422, 2017, 112–123.
- [4] Haq, R.U., Rashid, I., Khan, Z.H., Effects of aligned magnetic field and CNTs in two different base fluids over a moving slip surface, *Journal of Molecular Liquids*, 234, 2017, 682–688.
- [5] Rashid, I., Haq, R.U., Al-Mdallal, Q.M., Aligned magnetic field effects on water based metallic nanoparticles over a stretching sheet with PST and thermal radiation effects, *Physica E: Low-dimensional Systems and Nanostructures*, 89, 2017, 33–42.
- [6] Bilal, M., Nazeer, M., Numerical analysis for the non-Newtonian flow over stratified stretching/shrinking inclined sheet with the aligned magnetic field and nonlinear convection, *Archive of Applied Mechanics*, 91, 2021, 949–964.
- [7] Khashi'ie, N.S., Arifin, N.M., Rashidi, M.M., Hafidzuddin, E.H., Wahi, N., Magnetohydrodynamics (MHD) stagnation point flow past a shrinking/stretching surface with double stratification effect in a porous medium, *Journal of Thermal Analysis and Calorimetry*, 139, 2020, 3635–3648.
- [8] Khashi'ie, N.S., Arifin, N.M., Pop, I., Magnetohydrodynamics (MHD) boundary layer flow of hybrid nanofluid over a moving plate with Joule heating, *Alexandria Engineering Journal*, 61, 3, 2022, 1938–1945.
- [9] Srinivasulu, T., Goud, B.S., Effect of inclined magnetic field on flow, heat and mass transfer of Williamson nanofluid over a stretching sheet, *Case Studies in Thermal Engineering*, 23, 2021, 100819.
- [10] Saranya, S., Al-Mdallal, Q.M., Non-Newtonian ferrofluid flow over an unsteady contracting cylinder under the influence of aligned magnetic field, *Case Studies in Thermal Engineering*, 21, 2020, 100679.





- [11] Zhang, X.H., Abidi, A., Ahmed, A.E.S., Khan, M.R., El-Shorbagy, M.A., Shutaywi, M., Issakhov A., Galal, A.M., MHD stagnation point flow of nanofluid over a curved stretching/shrinking surface subject to the influence of Joule heating and convective condition, *Case Studies in Thermal Engineering*, 26, 2021, 101184.
- [12] Waini, I., Ishak, A., Pop, I., Nazar, R., Dusty hybrid nanofluid flow over a shrinking sheet with magnetic field effects, *International Journal of Numerical Methods for Heat & Fluid Flow*, 2021, <https://doi.org/10.1108/HFF-01-2021-0081>.
- [13] Waini, I., Ishak, A., Pop, I., Hybrid nanofluid flow over a permeable non-isothermal shrinking surface, *Mathematics*, 9, 2021, 538.
- [14] Waini, I., Ishak, A., Pop, I., MHD Glauert Flow of a Hybrid Nanofluid with Heat Transfer, *Journal of Advanced Research in Fluid Mechanics and Thermal Sciences*, 86, 2021, 91–100.
- [15] Ali, L., Liu, X., Ali, B., Mujeed, S., Abdal, S., Finite element analysis of thermo-diffusion and multi-slip effects on MHD unsteady flow of casson nano-fluid over a shrinking/stretching sheet with radiation and heat source, *Applied Sciences*, 9(23), 2019, 5217.
- [16] Ali, L., Liu, X., Ali, B., Finite Element Analysis of Variable Viscosity Impact on MHD Flow and Heat Transfer of Nanofluid Using the Cattaneo–Christov Model, *Coatings*, 10, 2020, 395.
- [17] Ali, L., Liu, X., Ali, B., Mujeed, S., Abdal, S., Khan, S.A., Analysis of Magnetic Properties of Nano-Particles Due to a Magnetic Dipole in Micropolar Fluid Flow over a Stretching Sheet, *Coatings*, 10, 2020, 170.
- [18] Ali, L., Wang, Y., Ali, B., Liu, X., Din, A., Mdallal, Q.A., The function of nanoparticle's diameter and Darcy-Forchheimer flow over a cylinder with effect of magnetic field and thermal radiation, *Case Studies in Thermal Engineering*, 28, 2021, 101392.
- [19] Ali, B., Naqvi, R.A., Ali, L., Abdal, S., Hussain, S., A comparative description on time-dependent rotating magnetic transport of a water base liquid H₂O with hybrid nano-materials Al₂O₃-Cu and Al₂O₃-TiO₂ over an extending sheet using Buongiorno model: Finite element approach, *Chinese Journal of Physics*, 70, 2021, 125–139.
- [20] Ali, L., Liu, X., Ali, B., Mujeed, S., Abdal, S., Mutahir, A. The Impact of Nanoparticles Due to Applied Magnetic Dipole in Micropolar Fluid Flow Using the Finite Element Method, *Symmetry*, 12, 2020, 520.
- [21] Ali, L., Wang, Y., Ali, B., Liu, X., Din, A., Mdallal, Q.A., The function of nanoparticle's diameter and Darcy-Forchheimer flow over a cylinder with effect of magnetic field and thermal radiation, *Case Studies in Thermal Engineering*, 28, 2021, 101392.
- [22] Deshpande, A.P., Krishnan, J.M., Kumar, P.B.S., *Rheology of complex fluids*, Springer, New York, 2010.
- [23] Kapur, J.N., Gupta, R.C., Two dimensional flow of Reiner-Philippoff fluids in the inlet length of a straight channel, *Applied Scientific Research*, 14, 1964, 13–24.
- [24] Cavatorta, O.N., Tonini, R.D., Dimensionless velocity profiles and parameter maps for non-Newtonian fluids, *International Communications in Heat and Mass Transfer*, 14, 1987, 359–369.
- [25] Hansen, A.G., Na, T.Y., Similarity solutions of laminar, incompressible boundary layer equations of non-newtonian fluids, *Journal of Basic Engineering*, 90, 1968, 71–74.
- [26] Na, T.Y., Boundary layer flow of Reiner-Philippoff fluids, *International Journal of Non-Linear Mechanics*, 29, 1994, 871–877.
- [27] Timol, M.G., Kalthia, N.L., Similarity solutions of three-dimensional boundary layer equations of non-Newtonian fluids, *International Journal of Non-Linear Mechanics*, 21, 1986, 475–481.
- [28] Patel, V., Timol, M.G., Similarity solutions of the three dimensional boundary layer equations of a class of general non-Newtonian fluids, *International Journal of Non-Linear Mechanics*, 21, 1986, 475–481.
- [29] Patil, V.S., Patil, N.S., Timol, M.G., A remark on similarity analysis of boundary layer equations of a class of non-Newtonian fluids, *International Journal of Non-Linear Mechanics*, 71, 2015, 127–131.
- [30] Yam, K.S., Harris, S.D., Ingham, D.B., Pop I., Boundary-layer flow of Reiner-Philippoff fluids past a stretching wedge, *International Journal of Non-Linear Mechanics*, 44, 2009, 1056–1062.
- [31] Ahmad, A., Qasim, M., Ahmed, S., Flow of Reiner–Philippoff fluid over a stretching sheet with variable thickness, *Journal of the Brazilian Society of Mechanical Sciences*, 39, 2017, 4469–4473.
- [32] Reddy, M.G., Sudharani, M.V.V.N.L., Kumar, K.G., Chamkha, A.J., Lorenzini, G., Physical aspects of Darcy-Forchheimer flow and dissipative heat transfer of Reiner–Philippoff fluid, *Journal of Thermal Analysis and Calorimetry*, 141, 2020, 829–838.
- [33] Kumar, K.G., Reddy, M.G., Sudharani, M.V.V.N.L., Shehzad, S.A., Chamkha, A.J., Cattaneo–Christov heat diffusion phenomenon in Reiner–Philippoff fluid through a transverse magnetic field, *Physica A: Statistical Mechanics and its Applications*, 541, 2020, 123330.
- [34] Ahmad, A., Flow of ReinerPhilippoff based nano-fluid past a stretching sheet, *Journal of Molecular Liquids*, 219, 2016, 643–646.
- [35] Reddy, M.G., Rani, S., Kumar, K.G., Seikh, A.H., Rahimi-Gorji M., Sherif E.S.M., Transverse magnetic flow over a Reiner–Philippoff nanofluid by considering solar radiation, *Modern Physics Letters B*, 33, 2019, 1950449.
- [36] Sajid, T., Sagheer, M., Hussain, S., Impact of temperature-dependent heat source/sink and variable species diffusivity on radiative Reiner–Philippoff fluid, *Mathematical Problems in Engineering*, 2020, 2020, 9701860.
- [37] Rosseland, S., *Astrophysik und atom-theoretische Grundlagen*, Springer-Verlag, Berlin, 1931.
- [38] Merkin, J.H., On dual solutions occurring in mixed convection in a porous medium, *Journal of Engineering Mathematics*, 20, 1986, 171–179.
- [39] Weidman, P.D., Kubitschek, D.G., Davis, A.M.J., The effect of transpiration on self-similar boundary layer flow over moving surfaces, *International Journal of Engineering Science*, 44, 2006, 730–737.
- [40] Harris, S.D., Ingham, D.B., Pop, I., Mixed convection boundary-layer flow near the stagnation point on a vertical surface in a porous medium: Brinkman model with slip, *Transport in Porous Media*, 77, 2009, 267–285.
- [41] Shampine, L.F., Gladwell, I., Thompson, S., *Solving ODEs with MATLAB*, Cambridge University Press, Cambridge, 2003.
- [42] Cortell, R., Heat and fluid flow due to non-linearly stretching surfaces, *Applied Mathematics and Computation*, 217, 2011, 7564–7572.
- [43] Ferdows, M., Uddin, M.J., Afify, A.A., Scaling group transformation for MHD boundary layer free convective heat and mass transfer flow past a convectively heated nonlinear radiating stretching sheet, *International Journal of Heat and Mass Transfer*, 56, 2013, 181–187.
- [44] Waini, I., Ishak, A., Pop, I., Hybrid nanofluid flow and heat transfer over a nonlinear permeable stretching/shrinking surface, *International Journal of Numerical Methods for Heat & Fluid Flow*, 29, 2019, 3110–3127.


ORCID iD

Iskandar Waini  <https://orcid.org/0000-0002-9883-5473>

Abdul Rahman Mohd Kasim  <https://orcid.org/0000-0001-9359-428X>

Najiyah Safwa Khashi'ie  <https://orcid.org/0000-0002-9092-8288>

Nurul Amira Zainal  <https://orcid.org/0000-0003-3045-302X>

Anuar Ishak  <https://orcid.org/0000-0002-2353-5919>

Ioan Pop  <https://orcid.org/0000-0002-0660-6543>



© 2022 Shahid Chamran University of Ahvaz, Ahvaz, Iran. This article is an open access article distributed under the terms and conditions of the Creative Commons Attribution-NonCommercial 4.0 International (CC BY-NC 4.0 license) (<http://creativecommons.org/licenses/by-nc/4.0/>).

How to cite this article: Waini I., Mohd Kasim A.R., Khashi'ie N.S., Zainal N.A., Ishak A., Pop I. Insight into Stability Analysis on Modified Magnetic Field of Radiative Non-Newtonian Reiner–Philippoff Fluid Model, *J. Appl. Comput. Mech.*, 8(2), 2022, 745–753. <https://doi.org/10.22055/JACM.2022.38820.3287>

Publisher's Note Shahid Chamran University of Ahvaz remains neutral with regard to jurisdictional claims in published maps and institutional affiliations.

